ELSEVIER

Contents lists available at ScienceDirect

Carbohydrate Polymers

journal homepage: www.elsevier.com/locate/carbpol



Structural features and immunological perception of the cell surface glycans of *Lactobacillus plantarum*: a novel rhamnose-rich polysaccharide and teichoic acids



Pilar Garcia-Vello^{a,1}, Garima Sharma^{b,1}, Immacolata Speciale^{a,c}, Antonio Molinaro^{a,c}, Sin-Hyeog Im^{b,*}, Cristina De Castro^{c,d,**}

- a Department of Chemical Sciences, University of Naples, 80126, Naples, Italy
- b Division of Integrative Biosciences and Biotechnology, Department of Life Sciences, Pohang University of Science and Technology (POSTECH), Pohang, 37673, Republic of Korea
- ^c Task Force on Microbiome Studies, University of Naples Federico II, Naples, Italy
- ^d Department of Agricultural Sciences, University of Naples, 80055 Portici, Italy

ARTICLE INFO

Keywords: Capsular polysaccharide Teichoic acid Structure Immunological activity NMR

ABSTRACT

The capsular material from *Lactobacillus plantarum* IMB19, an isolate from fermented vegetables, has been analyzed and our results demonstrate that most of the coat of this bacterium consists of glycerol- and ribitol-type teichoic acids, further decorated with other substituents (α -glucose and alanine), and of a capsular polysaccharide (CPS) with a linear nonasaccharide repeating unit, rich in rhamnose, interconnected to the next via a phosphodiester bridge.

Stimulation of immune cells with the total capsular material resulted in the enhancement of immunostimulatory (IFN γ , TNF- α , IL-6 and IL-12) or immuno-regulatory (IL-10) cytokines in an *in vitro* splenocyte culture system. The capsular polysaccharide, and not the teichoic acids mixture, was responsible for the IFN γ production. Indeed, a significant increase of IFN γ along with other inflammatory cytokines, and a dose response in IFN γ expression with an EC₅₀ of 3.16 μ M was found for CPS, disclosing that this polysaccharide is a potent immunostimulatory molecule.

1. Introduction

The earliest exploration of capsular polysaccharide diversity was done as part of a broader research programme to classify bacteria based on the interaction of their cell surface antigens with human sera (Lancefield, 1933). Extensive research in the field of probiotics, i.e beneficial commensal bacteria, has shown that commensals derived polysaccharides affect not only host health but also have potential as candidates for adjunct therapy in several disease conditions. Capsular polysaccharides (CPSs) present on some of the commensals like *Bacteroides fragilis* and *Bifidobacterium bifidum* PRI1 have been specifically linked to beneficial effects to the host immune system (Speciale et al., 2019; Telesford et al., 2015; Verma et al., 2018). The *Lactobacillus* genus of bacteria forms a significant component of the commensal microflora at various mucosal sites of the human body. *Lactobacilli* are

widely used as probiotics and have "Generally Recognized As Safe (GRAS)" status, and several of these strains have been investigated for their beneficial effects to the host (Kwon et al., 2010; Chae, Kwon, Hwang, Kim, & Im, 2012; Baarlen, Wells, & Kleerebezem, 2013; Rocha-Ramírez et al., 2017). Genetically, *Lactobacilli* are known to carry gene clusters for exopolysaccharide or capsular polysaccharide synthesis (Zeidan et al., 2017), and the beneficial effects of these "friendly *Lactobacilli*" have been proposed to be in part due to these surface molecules (Kleerebezem et al., 2010).

The structure to function relationship of the CPSs from *Lactobacillus plantarum* has been relatively less explored compared to other *Lactobacillus species*. A few studies have observed that the immunological effects of *L. plantarum* CPSs are strain specific (Lee et al., 2016; Remus et al., 2012). Distinct functional effects of *L. plantarum* WCFS1 CPS co-administered with those from *L. rhamnosus* LOCK 900

^{*} Corresponding author.

^{**} Corresponding author at: Department of Agricultural Sciences, University of Naples, 80055 Portici, Italy E-mail addresses: iimsh@postech.ac.kr (S.-H. Im), decastro@unina.it (C. De Castro).

¹ Equal contribution.

were observed on bone marrow derived dendritic cells and depending on the specific CPS fraction from *L. rhamnosus* used in co-administration, immune-regulation or immune-stimulation effects were observed, as reflected by the excreted cytokines (Górska et al., 2014). Hence, capsular polysaccharides appear to be involved in the interactions between the microbes and the host, with the ability to tune the immunological response thus contributing to the host's health status. Thus, the knowledge of the structure of the polysaccharides can provide a framework for defining the immunological properties.

Here, we focused our study on *L. plantarum* IMB19, an isolate from *Kimchi* (a traditional fermented vegetable preparation used in Korean food) to understand which beneficial effects, if any, derive from the bacterial capsule. Our analysis discloses that the bacterial surface is coated with teichoic acids (TA), as expected for a Gram-positive bacterium, and a novel rhamnose rich capsular polysaccharide. Along with the detailed investigation of the CPS structure, we evaluated the effect of both components on murine immune cells to unveil their immunological potential.

2. Materials and methods

2.1. Bacterial growth and crude polysaccharide isolation

L. plantarum IMB19 (Lp IMB19) was isolated from Kimchi, by selecting colonies obtained from culture in De Man, Rogosa and Sharpe (MRS) broth (Becton-Dickinson, USA) for 48 h. Selected colonies were identified based on the 16s rRNA sequencing analysis (Macrogen, S.Korea). Sequence similarity was confirmed using BLAST tool by NCBI. Lp IMB19 was distinguished from other genotypically closely related species by amplification of recA gene using recA gene-derived primers, as reported earlier (Torriani, Felis, & Dellaglio, 2001). Lp IMB19 was typically cultured in MRS broth at 37 °C for 24-36 h, and its morphology along with the presence of a capsular coat, was evaluated by cryosection transmission electron microscopy (TEM), as described earlier (Kang et al., 2013). For CPS isolation, the bacterium was cultured in semi-defined media (SDM), as described (Sanchez, Martinez, Guillen, enez-D1az, & Rodriguez, 2006). CPS isolation and purification was done using a modification of a method previously described (Verma et al., 2018) which consisted of detachment of the capsular material from the cells by sonication, precipitation of the supernatant with ethanol followed by resuspension of the solid in TRIS buffer to carry on enzymatic treatment to remove protein and nucleic acids. The detailed protocol used to obtain the total CPS fraction, together with the conditions used for transmission electron microscopy are reported in full in the Supporting Information.

2.2. Polysaccharides chemical analyses

Monosaccharide content analysis as acetylated methylglycosides, and absolute configuration determination as acetylated octylglycosides, was performed as reported (De Castro, Parrilli, Holst, & Molinaro, 2010). Identification of the derivatives was inferred by GC–MS analysis by comparing the retention time of the peaks in the sample with that from in-house built standards, under the condition listed in Supporting Information.

The dephosphorylation reaction was performed by dissolving the sample (500 μ g) in HF 50 % (50 μ L, 48 h, 4 °C). The solution was dried with a stream of air, suspended in water (50 μ l) and dried under airflow at 40 °C. This procedure was repeated twice, and then the sample was transformed in the corresponding acetylated methylglycosides.

2.3. Chromatographic purification

The total CPS fraction (28 mg) was purified via anion exchange Q-Sepharose fast flow chromatography (GE Healthcare; $V=4.4\,\mathrm{mL}$, flow 16 mL/h). The resin was packed and washed in 1 M NaCl, then

equilibrated with 10 volumes of NaCl 10 mM. Then CPS was dissolved in 10 mM NaCl (5 mL) and adsorbed on the resin. The elution was realized stepwise by adding sequentially $16\,\mathrm{mL}$ of NaCl: 10, 100, 200, 400, 700 and $1000\,\mathrm{mM}$. The eluate corresponding to each solution was collected, desalted by dialysis (cut-off $1000\,\mathrm{Da}$), and freeze-dried. The six fractions were labeled CPS-x, with x indicating the NaCl concentration (mM) used for elution.

The molecular weight determination was inferred for CPS-100 and CPS-400 by using an HPLC system Agilent 1100 HPLC system, with a TSK G-5000 PW_{XL} size exclusion column (30 cm \times 7.8 mm) equilibrated with NH₄HCO₃ 50 mM as eluent (flow = 0.8 mL/min) and the eluate was monitored with a refractive index detector. The column was calibrated by injecting dextran standards (50 μ L of a 1 mg/mL solution) of known molecular weight (12, 50, 150, and 670 kDa); the Log of the molecular weight was plotted against the elution volume, and the linear relationship found (LogMW = -0.811 mL + 11.7; R^2 = 0.98) was used to calculate the MW of the two fractions (Speciale et al., 2019).

2.4. NMR acquisition parameters

For structural assignments of the isolated polysaccharides, NMR spectra were recorded in D_2O by using a Bruker 600 MHz spectrometer equipped with a reverse cryo-probe with gradients along the z-axis. The NMR sequences used for structural elucidation were: ($^1H^{-1}H$ homonuclear) DQ-COSY (double quantum COSY spectrum, hereafter referred as COSY), TOCSY, and NOESY, ($^1H^{-13}C$ heteronuclear) HSQC, HMBC, and HSQC-TOCSY. All the spectra were calibrated with acetone as internal standard (1H 2.225 ppm; ^{13}C 31.45 ppm), acquired with Topspin 2.0 software (Bruker), processed and studied with Topspin 3.6. Details on execution of the spectra are given in the Supporting Information.

2.5. Splenocyte culture assay for immunological assessment

All animal experiments and procedures were performed in compliance with ethical regulations and approval of the POSTECH University Institutional Animal Care and Use Committee. C57BL/6 mice were housed in a pathogen-free animal barrier facility, bred in-house and used at 6-8 weeks age. Spleens were harvested and gently crushed to release splenocytes. Cell suspension was subjected to RBC (Red Blood Cell) lysis using ammonium chloride buffer and resuspended in complete RPMI media (Welgene, S. Korea) supplemented with 10 % FBS (Hy-Clone, Australia). Cells were plated at a density of 200,000 k/well in 200 μL media/well containing anti-CD3 (Bio-Xcell, USA) $10\,ng/mL$ and GM-CSF (Peprotech, USA) 2.5 ng/mL in a 96 well plate. Fractionated CPS-100 and CPS-400, total unfractionated CPS, LPS (lipopolysaccharide from E-coli 0111:B4, Invivogen, USA) and media were added as required and incubated for 48 h at 37 °C, 5 % CO₂. Supernatants were collected after centrifugation and frozen for use in later cytokine estimation by Enzyme linked immunosorbent Assay (e-Bioscience, Ready set go ELISA kits), as per the manufacturer's instructions.

3. Results

3.1. Chemical characterization of the crude polysaccharide fraction

L. plantarum IMB19 analysis by transmission electron microscopy disclosed that the cells were surrounded by a consistent layer of a capsular substance (Fig. S1), whose carbohydrate composition consisted of rhamnose, galactose, glucose and glucosamine, and minor amounts of glycerol and ribitol (Fig. S2a). These two polyols are generally associated with the presence of teichoic acids (Tomita, Tanaka, & Okada, 2017), where they are interconnected through phosphodiester linkages. Normally these polyols are poorly detected because methanolysis is unable to completely cleave the phosphodiester linkage. Hence, the analysis was repeated by dephosphorylating the sample with

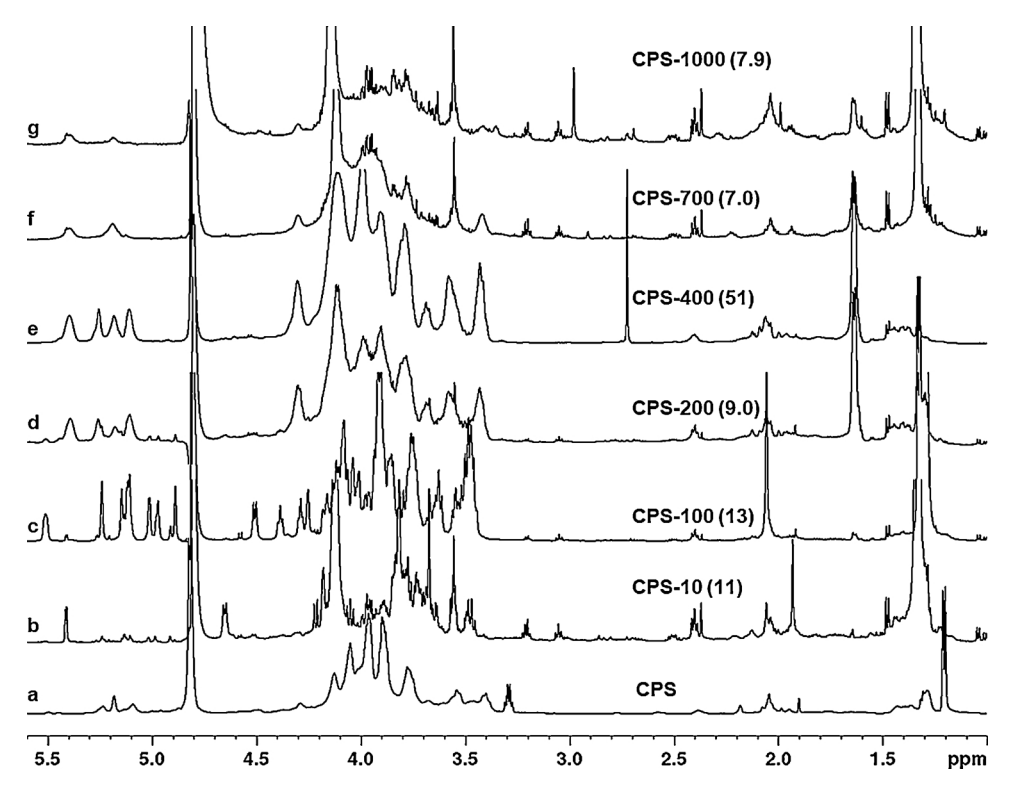


Fig. 1. (600 MHz, 298 K) Proton spectra recorded for the fractions obtained by purification of the crude CPS via ion exchange chromatography. a) CPS, b) CPS-10, c) CPS-100, d) CPS-200, e) CPS-400, f) CPS-700, and g) CPS-1000. Numbers reported in brackets indicate the yields (mg/mg) of each fraction starting from 28 mg of crude CPS.

aqueous HF prior to methanolysis and acetylation, and the relative amount of both polyols increased (Fig. S2b), confirming the presence of teichoic acid. As for the monosaccharides, rhamnose had the L absolute configuration, glucose and galactose were D (Fig. S3), while for glucosamine the D configuration was assumed based on the exclusive presence in nature of this stereoisomer.

3.2. Purification of the crude polysaccharide

The results of carbohydrate composition suggested that CPS could be a mixture of polymers. Accordingly, purification by ion exchange chromatography was performed and the six fractions obtained were labeled as CPS-x depending on the concentration of the eluent used. The following yields were observed: CPS-10 11 %, CPS-100 13 %, CPS-200 9.0 %, CPS-400 51 %, CPS-700 7.0 %, and CPS-1000 7.9 %, each fraction was compared to the spectrum profile of the original mixture (Fig. 1a) by $^1\mathrm{H}$ NMR analysis (Fig. 1).

Overall, the isolation of different components was achieved (Fig. 1). CPS-10 appeared rather heterogenous (Fig. 1b): its anomeric region contained two main signals not in scale with the intense signals at 4.2 and 1.3 ppm, associated to material different from carbohydrates; given the low amount of material recovered, this fraction was not considered for further studies.

As for CPS-100 (Fig. 1c), the anomeric region (5.6-4.5 ppm) contained nine major signals, with that at 5.5 ppm, appearing as a double doublet (better visible in Fig. 2), which suggested that it was a residue in the α -configuration ($^3J_{\rm H1,H2}=3.4\,\rm Hz$) and phosphorylated ($^3J_{\rm H1,P}=7.0\,\rm Hz$). Further, it was noted the presence of an acetyl group (methyl group at 2.06 ppm) and of an intense signal including several methyl groups of 6-deoxyresidues (1.3 ppm), in agreement with the presence of N-acetylglucosamine and rhamnose units, respectively.

Fraction CPS-200 (Fig. 1d) appeared as a mixture of CPS-100 and CPS-400 (Fig. 1e), which in turn presented four, rather broad, signals in the anomeric region, an intense methyl signal at 1.6 ppm (a value not consistent with the methyl of rhamnose) and a crowded carbinolic region (4.4-3.2 ppm). By integration, the ratio between anomeric and carbinolic protons was 1.0: 12, while the ratio usually expected is 1:6

(or less) suggesting that CPS-400 did not have the structure typical of a polysaccharide and that the increase in the ratio observed was due to the presence of ribitol and glycerol units, as confirmed by its chemical analysis (Fig. S4). Moreover, glucose was the most abundant monosaccharide followed by small amounts of glucosamine (GlcN) and muramic acid (MurA), two monosaccharides characteristic of the peptidoglycan. This finding supported the notion that CPS-400 was teichoic acid (TA).

As for CPS-700 and CPS-1000 (Figs. 1f and g, respectively), the anomeric region contained only some of the signals found in CPS-400, and in both cases there was an atypical ratio of anomeric versus carbinolic protons, in addition to signals from non-carbohydrate material. Given the low abundance along with the concerns about purity, these two fractions were not investigated further.

3.3. NMR analysis of CPS-100

The structure of the capsular polysaccharide was determined by analyzing the complete set of $^1\text{H-}^1\text{H}$ homonuclear (COSY, TOCSY, NOESY) and $^1\text{H-}^{13}\text{C}$ heteronuclear (HSQC, HMBC, HSQC-TOCSY) 2D NMR spectra recorded at 310 K (attributions in Table 1). The rise in temperature from 298 K (Fig. 1c) to 310 K (Fig. 2) reduced the overlap between the three anomeric signals at ca. 5.15 ppm and simplified the NMR attribution of the related residues.

The HSQC spectrum (Fig. 2) presented nine main anomeric densities at ^1H 5.6–4.5 ppm that were labeled with a capital letter (A-I, Fig. 2a, Table 1), while the corresponding protons had all similar proportions. NMR analysis started from H-1 of A (5.51 ppm) that displayed three correlations in the TOCSY spectrum (Fig. 3), with that at 3.85 ppm in common with the COSY spectrum. Hence, this density was assigned to H-2, and by a similar approach, H-3 (3.91 ppm) and H-4 (4.04 ppm) were also assigned. Lack of further correlations from H-1 enabled the recognition of A as a galactose unit. H-5 was identified in the NOESY spectrum through its intense H-4/H-5 correlation (Fig. 4), and it enabled the finding of the two H-6 s via the corresponding COSY correlation (Figs. 3 and 4).

HSQC and the HSQC-TOCSY spectra (Fig. 5a) defined all the carbon

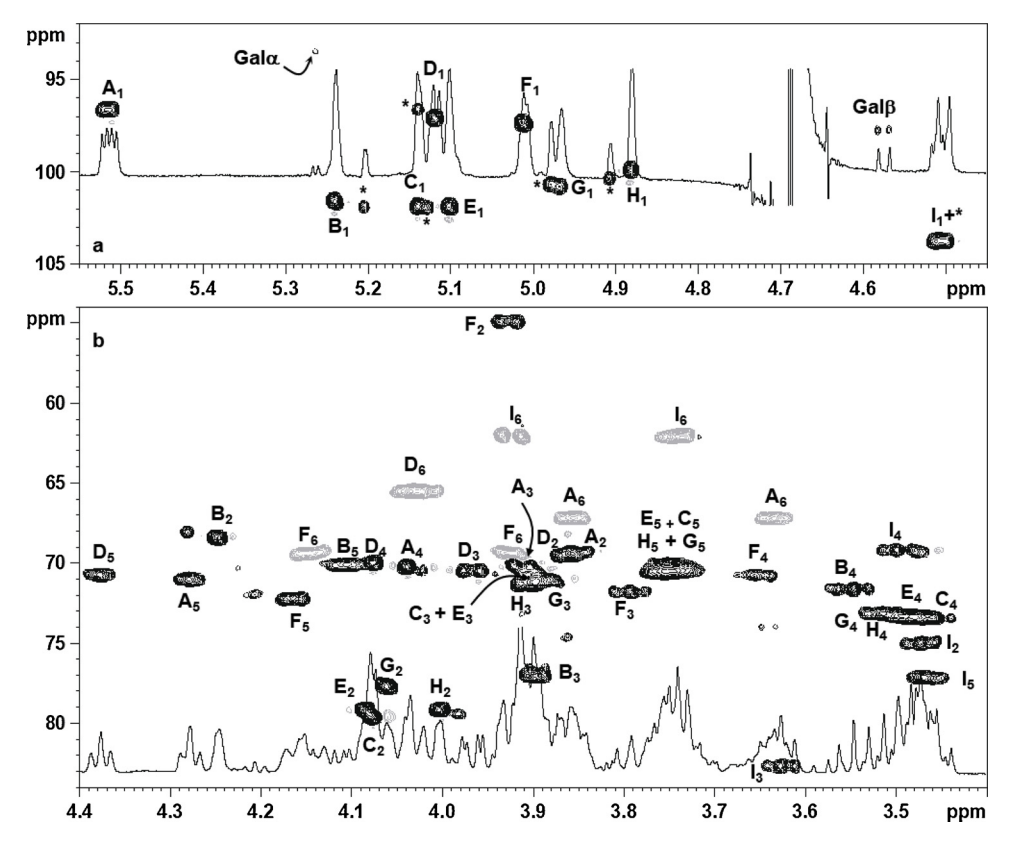


Fig. 2. (600 MHz, 310 K) Expansion of HSQC spectrum recorded for the capsular polysaccharide from L. *plantarum* IMB19, a) expansion of the anomeric region; b) expansion of the carbinolic area. Grey densities correspond to "CH₂" carbons. "*" refers to minor anomeric signals of sugars of the repeating unit attached to a galactose in the reducing form (Gal α and Gal β). The structure of the repeat is reported in Fig. 6 and labels refer to Table 1.

Table 1 (600 MHz, 310 K) Proton (¹H, plain text) and carbon (¹³C, italic) NMR chemical shifts of the repeating unit (Fig. 6) of the capsular polysaccharide from *Lactobacillus plantarum* IMB19.

	1	2	3	4	5	6
A	5.51	3.85	3.91	4.04	4.28	3.86;3.63
6-α-Gal-1 <i>P</i>	96.6	69.3	70.2	70.2	71.1	67.1
В	5.24	4.25	3.90	3.55	4.11	1.29
3-α-Rha	101.6	68.4	77.1	71.7	70.2	18.1
C	5.14	4.08	3.90	3.46	3.73	1.29
2-α-Rha	101.9	79.6	ca 71*	73.4	ca 70.5**	18.1
D	5.12	3.86	3.97	4.08	4.38	4.04;4.02
6P-α-Gal	97.1	69.5	70.4	70.0	70.8	65.6
E	5.10	4.08	3.90	3.48	3.76	1.29
2-α-Rha	101.9	79.2	ca 71*	73.4	ca 70.5**	18.1
F	5.01	3.93	3.79	3.65	4.17	4.14;3.92
6-α-GlcNAc	97.4	54.9	71.8	70.7	72.3	69.5
G	4.97	4.06	3.89	3.52	3.76	1.29
2-α-Rha	100.8	77.8	71.1	73.2	ca 70.5**	18.1
Н	4.88	4.00	3.91	3.48	3.75	1.31
2-α-Rha	99.9	79.2	71.4	73.3	ca 70.5**	18.1
I	4.50	3.47	3.63	3.50	3.46	3.92;3.74
3-β-Glc	103.7	75.0	82.8	69.1	77.2	62.1

 $^{^{\}ast}\,$ C-3 of C and E are overlapped, and their precise chemical shift could not be determined with certainty.

chemical shifts of A (Table 1), an α -galactose unit linked at O-6 based on the high chemical shift of C-6 (67.1 ppm).

Correlations on the TOCSY spectrum originating from H-1 (5.12 ppm) of **D**, had the same pattern of **A**, hence **D** was also a galactose, α configured based on the $^3J_{\rm H1,H2}$ (3.9 Hz) value, and the chemical shift of H-6 s/C-6 (4.04-4.02/65.6 ppm) disclosed that this position was phosphorylated in agreement with literature data (Sechenkova et al., 2004). Therefore, **D** was a 6*P*- α -Gal, not further branched based on high field values of all the other carbon chemical

shifts

As for **B**, H-1 (5.24 ppm) displayed two TOCSY correlations with the most intense attributed to H-2 (4.25 ppm) and this was coincident with the COSY density (Fig. 3). Reading of the TOCSY from this second proton (Fig. 3) identified all the other protons of the unit including a methyl at 1.28 ppm (not shown), a pattern overall diagnostic of a rhamnose residue. Hence, **B** was a rhamnose α -configured at the anomeric center based on the similarity of its C-5 value (ca. 70.5 ppm) with that of the reference glycoside (69.4 or 73.6 ppm for α or β methylglycosides, respectively, Bock & Pedersen, 1983) and 3-substituted as defined from the glycosylation shift experienced from the corresponding carbon.

The TOCSY pattern of the residues **C**, **E**, **G** and **H** (H-1 at 5.14, 5.10, 4.97, 4.88 ppm, respectively) was similar to that of **B**, indeed they were α -rhamnose units, and the low field value of their C-2 (77.8–79.6 ppm) compared to the reference value (71.0 ppm, Bock & Pedersen, 1983) disclosed that they were substituted at O-2.

As for F, H-1 (5.01 ppm) had four TOCSY correlations (Fig. 3), attributed to H-2 to H-5 with the aid of the COSY spectrum, a pattern diagnostic of a *gluco* configurated residue. HSQC-TOCSY analysis from H-5, identified a correlation with a density at 69.5 ppm, attributed to C-6 and in turn related to the H-6 s (4.14 and 3.96 ppm). Hence, F was a N-acetylglucosamine based on the C-2 (54.9 ppm) and H-2 (3.93 ppm) values and substituted at C-6 (69.4 ppm). The α configuration was inferred by the shape of the anomeric signal (broad singlet) and by the C-3 value (71.8 ppm), very similar to that of the reference α -glycoside (72.0 ppm, Bock & Pedersen, 1983).

Finally, H-1 of I (4.50 ppm) had a TOCSY pattern which identified all the protons of the unit. Hence, based on the 13 C chemical shifts, I was a glucose, substituted at C-3 (82.8 ppm) and β -configurated based on the $^{3}J_{\rm H1,H2}$ value (7.9 Hz).

The sequence between the residues was deduced by analyzing the HMBC (Fig. 5b) and NOESY (Fig. 4) spectra. First, correlations on the HMBC (Fig. 5b) connected H-1 of B with C-3 of I and the corresponding density was labeled B_1I_3 . By the same formalism, these other

 $^{\,\,^{**}\,}$ C-5 of C, E, G and H are overlapped, and their precise chemical shift could not be determined with certainty.

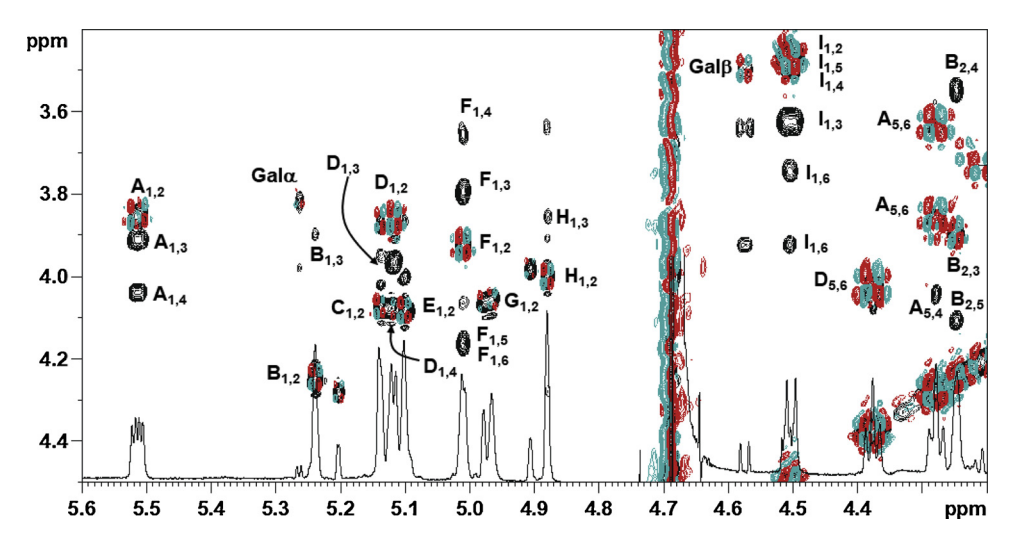


Fig. 3. (600 MHz, 310 K) Expansion of TOCSY (black) and COSY (cyan/red) spectra recorded for CPS-100 the capsular polysaccharide of *L. plantarum* IMB19. The structure of the repeat is reported in Fig. 6 and labels refer to Table 1. (For interpretation of the references to colour in this figure legend, the reader is referred to the web version of this article).

correlations were found: C_1E_2 , D_1B_3 , F_1G_2 , H_1A_6 and I_1F_6 . Furthermore, H-1 of E and H-1 of G had a long-range correlation with a carbon at ca. 79 ppm, a value similar to C-2 of C and H. The correct assignment of these densities as E_1H_2 and G_1C_2 , was inferred by analyzing the NOESY spectrum (Fig. 4) which related H-1 of E with H-2 of H, and H-1 of G with H-2 of C. These attributions were confirmed by observing the reverse correlations, as detailed in the expansion of the H-2 protons of the different rhamnose units (Fig. S5).

Finally, the information that **A** and **D** were phosphorylated (at O-1 and O-6, respectively), led to join them through a phosphodiester linkage, which explained why no HMBC connectivity appeared for H-1 of **A** and C-6 of **D**, or for H6 of **D** and C-1 of **A**, or why none of these protons had an inter-residue NOE correlation. Actually, HMBC spectrum could not detect any correlation between the two units because the number of bonds between the H-1 (or C-1) of **A** and C-6 (or H-6s) of **D** (five linkages) is much beyond the limit (three linkages) of this sequence. Similarly, the phosphate moiety between **A** and **D**, keeps the protons of these units too far apart from each other for giving a detectable NOE effects.

Hence, the structure of the repeating unit of CPS-100 is a non-asaccharide as reported in Fig. 6.

Additionally, we investigated the minor NMR signals to understand their nature. In the HSQC spectrum (Fig. 2), the carbon chemical shifts of the densities labeled as Gal α and Gal β ($^1\text{H}/^{13}\text{C}$ 5.26/93.5 and 4.57/97.8 ppm, respectively) were indicative of α or β residues in the free reducing form. Inspection of the TOCSY spectrum (Fig. 3) from their H-1 showed the pattern typical of *galacto* configured sugars (namely three

densities, for $Gal\alpha$ the third density almost overlapped with the COSY density). This finding was explained by considering that the procedure used to isolate the CPS included sonication and trichloroacetic acid treatment, both able to induce some cleavage of the phosphodiester linkage, especially on the side of anomeric phosphate of the galactose A because of the extreme lability of this bond.

Accordingly, it was hypothesized that the minor signals next to the intense signals (Fig. 2, labelled with a "*"), belonged to residues of the first repeat and that were connected to the galactose in the free reducing form. However, their low intensity and the crowding in the carbinolic region prevented the precise attribution. Finally, by integration of the anomeric densities in the HSQC spectrum (Fig. 2a), it was possible to evaluate that the averaged degree of polymerization of the sample was four, and the averaged MW of about 6 kDa (MW of the repeating unit is 1500 Da), a value similar to that, slightly overestimated, calculated by HPSEC of 11 kDa (Fig. S6).

3.4. NMR analysis of CPS-400

An approach similar to that described for CPS-100 was used to unravel the structural features of CPS-400 (Table 2). First, the anomeric region (Fig. 7a,b) of the HSQC spectrum displayed several signals, with those at ^1H 5.3-5.1 ppm arising from monosaccharide residues, while that at $^1\text{H}/^{13}\text{C}$ 5.39/75.5 ppm was not an anomeric signal, but the C-2 of a glycerol unit (Gro), labeled **A**, and shifted to low field by acylation. The substituent at O-2 was an alanine (Ala), identified by the diagnostic methyl at $^1\text{H}/^{13}\text{C}$ 1.64/16.5 ppm and by its $\text{H}_{\alpha}/\text{C}_{\alpha}$ at 4.30/50.2 ppm.

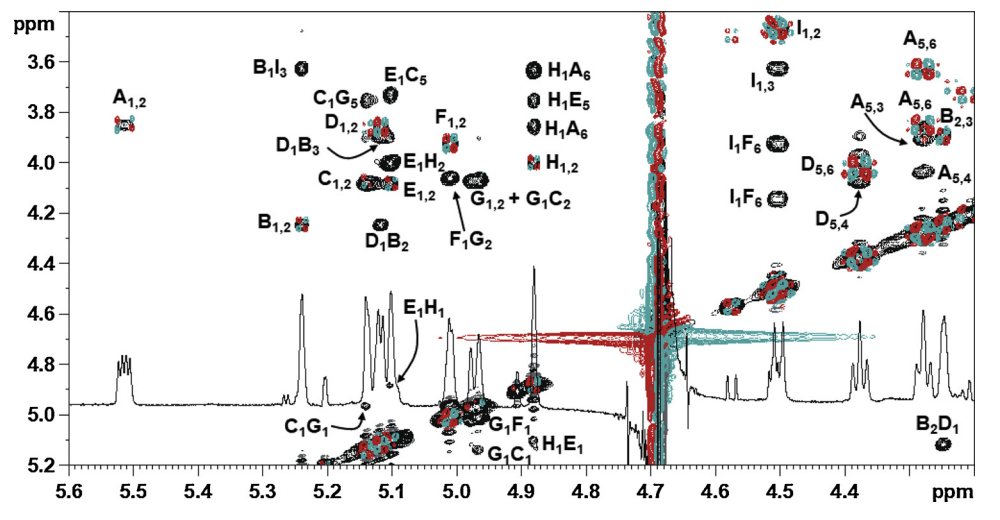


Fig. 4. (600 MHz, 310 K) Expansion of NOESY (black) and COSY (cyan/red) spectra recorded for CPS-100 the capsular polysaccharide of *L. plantarum* IMB19. The structure of the repeat is reported in Fig. 6 and labels refer to Table 1. (For interpretation of the references to colour in this figure legend, the reader is referred to the web version of this article).

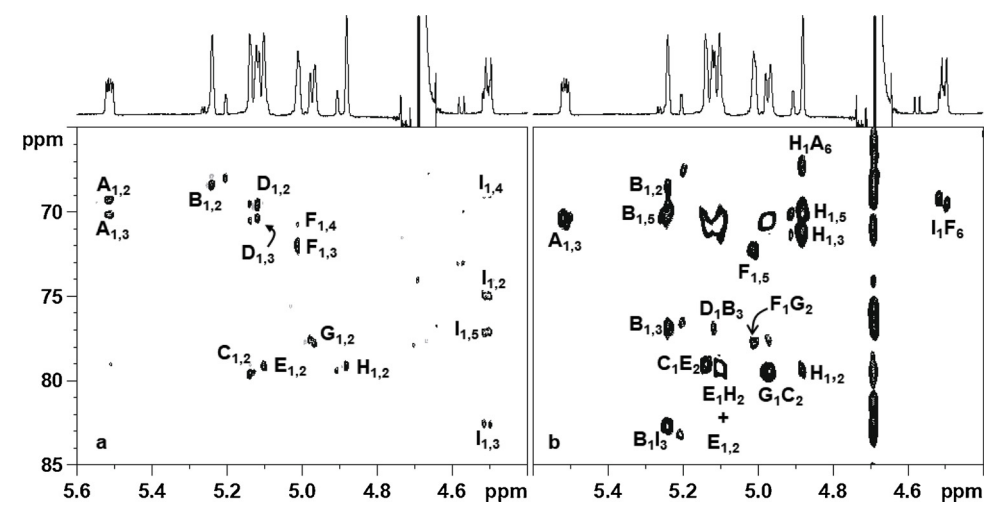


Fig. 5. (600 MHz, 310 K) Expansion of a) HSQC-TOCSY and b) HMBC NMR spectra recorded on the capsular polysaccharide from *L. plantarum* IMB19. The structure of the repeat is reported in Fig. 6 and labels refer to Table 1.

Further, H-1/C-1 and H-3/C-3 of **A** were equivalent and found at 4.11/65.0 ppm based on the corresponding HSQC-TOCSY (Fig. 7a) and TOCSY (Fig. 7g) correlations. Finally, C-1 (or C-3) value indicated that **A** was phosphorylated at both ends (Gerlach et al., 2018) as happens for Gro-type teichoic acids.

HSQC analysis aided by literature data (Gerlach et al., 2018) identified a second 1,3-diphosphorylated Gro unit (B), and also a 1,5-diphosphorilated ribitol unit (Rbo, C); this last residue suggested the presence of another teichoic acid based on a ribitol-phosphate backbone (Rbo-type TA).

As for the monosaccharide units, analysis focused on the most intense signals (D, E, F' and F) which were identified as α -glucose units, based on the efficient propagation of the magnetization from the anomeric signals up to H-6 in the TOCSY spectrum (Fig. 7g). These Glc units were not further substituted based on the similarity of their ^{13}C chemical shifts with those of the reference glycoside (Bock & Pedersen, 1983).

The location of these units was inferred by analyzing the HMBC spectrum and by comparison with literature data. Indeed, E was linked to O-2 of a Gro unit (H) (Shashkov, Potekina, Senchenkova, & Kudryashova, 2009), while F' was linked to O-4 of a Rbo unit (I) (Streshinskaya et al., 2011).

As for **D**, its H-1 had a long-range correlation with a carbon at 78.3 ppm (Fig. 5b) whose proton (4.30 ppm) was connected to a "CH₂" at 69.9 ppm in the HSQC-TOCSY spectrum (Fig. S7). This new unit was labeled **G** and the densities at $^1\text{H}/^{13}\text{C}$ 4.30/78.3 and 4.14/66.9 ppm were assigned to \textbf{G}_4 and \textbf{G}_5 , respectively (Figs. 5c and S7). **G** was identified as a ribitol and the finding of its other signals was possible by analyzing the HSQC-TOCSY spectrum. Indeed, the "CH₂" density at $^1\text{H}/^{13}\text{C}$ 4.16/67.7 ppm had three other correlations with one pointing to \textbf{G}_4 (Fig. S7), hence this density was labeled as \textbf{G}_1 . Further, C-1 of **G** (67.7 ppm) was diagnostic of a carbon phosphorylated and not glycosylated at the adjacent position, as reported for **I** (Table 2). This information made possible the assignment of the remaining two HSQC-TOCSY correlations to C-2 (70.5 ppm) and C-3 (80.6 ppm), which in turn identified the corresponding H-2 (4.15 ppm) and H-3 (3.97 ppm) in

the HSQC spectrum (Figs. 5 and S7, Table 2). Thus, **G** was a Rbo glucosylated at both O-3 and O-4 with **F** and **D** being the two units attached (HMBC in Fig. 7b).

This type of substitution was already identified in other *Lactobacillus plantarum* strains (Tomita et al., 2017) but the NMR data reported the Rbo unit devoid of the phosphates, so that these chemical shifts could not be compared with our data (Tomita et al., 2009). However, our attributions agreed with those of the TA from a *Bifidobacterium* (Valueva et al., 2013) for which the authors proposed a reversed substitution pattern, namely a ribitol with the glucose units linked at C-2, and C-3. Interestingly, the NMR data of the dephosphorylated form from Valueva et al. (2013) coincided with that of the 3,4-diglucosylated ribitol from Tomita et al. (2009), thus leaving the substitution pattern (2,3 or 3,4) of this ribitol unit yet to be univocally defined.

Therefore, our data identified CPS-400 as a mixture of two teichoic acids, the Gro- and Rbo-type, each presenting some substituents in a non-stoichiometric fashion. For the Gro-type TA, the non-stoichiometric substituents were Alanine and α -glucose. For the Rbo-type TA, α -glucose occurred at both O3 and O4 of ribitol, at O4 only or at neither position.

Our hypothesis of a mixture of two types of TAs is supported by the fact that some strains of *Bacilli* can produce both TA simultaneously (Brown, Santa Maria, & Walker, 2013), and by the knowledge that a strain of *L. plantarum* harbors the biosynthetic tools to produce both types of TAs (Bron et al., 2012).

To further support our hypothesis, we tried to separate the two TA species by size exclusion chromatography, but CPS-400 appeared as a single symmetrical peak of about 45 kDa (Fig. S6) hindering any possibility to proceed further in this direction. Separation of the two TAs will be addressed within future work.

3.5. Immunostimulant activity of CPS-100 and CPS-400

We assessed the functional characteristics of fractionated CPS *in vitro*, to emphasize its potential biological role in health and disease. Splenocytes, a mix of all immune cells in physiological ratio were used

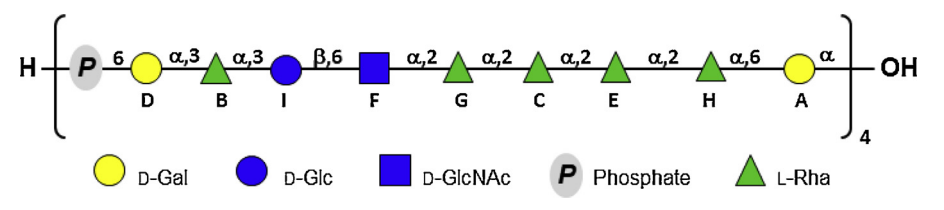


Fig. 6. Structure of the repeating unit of CPS-100, the capsular polysaccharide from L. *plantarum* IMB19; labels refer to Table 1.

Table 2 (600 MHz, 310 K) NMR data of CPS-400. Position 1 of ribitol (or glycerol) points to the right; the "motif" column depicts the structure of the unit and, in case of substituted Rbo or Gro units, it indicates the nature of the substituent and specifies its position.

Residue	motif	1	2	3	4	5	6
A	Ala O	4.11 × 2	5.39	4.11 × 2	-	-	-
	P P						
Gro	Ala	65.0	75.5	65.0	-	-	-
В	OH P	3.96;3.89	4.05	3.89; 3.96	-	-	-
Gro	× × × ×	67.5	70.8	67.5	_	_	_
С	он он	4.09; 4.00	3.99	3.81	3.99	4.09; 4.00	-
Rbo	P	67.8	72.2	72.5	72.1	67.8	-
D *	ÓН _{ОН}	5.17	3.57	3.80	3.43	4.00	3.90; 3.78
t-α-Glc	но	98.4	72.8	74.2	70.8	72.8	61.8
E*	OH	5.17	0.54	0.76	2.40	2.00	2.00. 2.70
E^ t-α-Glc	-0	5.17	3.54	3.76	3.42	3.92	3.90; 3.78 61.8
t-a-Gic	НОООН	99.0	72.7	74.2	71.0	73.1	01.8
F *	ОН	5.10	3.58	3.69	3.43	3.89	3.90; 3.78
t-α-Glc	HOOLOH	101.5	72.8	73.8	70.9	74.0	61.8
F'*	ОН	5.11	3.58	3.79	3.43	4.00	3.90; 3.78
	но он	98.7	72.8	74.2	70.9	72.8	61.8
G	Glc O OH	4.16 × 2	4.15	3.97	4.30	4.14 × 2	
	O Glc						
Rbo	(3 F;4D)	67.7	70.5	80.6	78.3	66.9	
Н	Glc	4.02**	4.11	4.05; 4.00**			
	PP						
Gro	2E	67.7	76.6	66.4			
I	Glc O OH	4.09; 4.00	3.92	3.99	4.12	4.15; 4.12	
Rbo	ÓH 4F'	67.8	71.2	70.9	79.0	65.8	
Ala		_	4.30	1.64			
		171.3	50.2	16.5			

^{*} For all these residues, the H-6/C-6 are coincident.

to obtain a comprehensive effect of CPS on the immune system. Endpoint analysis was performed by testing for different cytokines by ELISA. Cytokines are a group of secretory peptides/glycoproteins involved in cell signaling which mediate as well as regulate inflammatory or tolerogenic immune response in vivo. Hence, skewing of cytokines in a pool of immune cells on exposure to CPS implies its similar role in vivo. Here, we analyzed interferon gamma (IFNγ) as an inflammatory marker and interleukin-10 (IL-10) as a regulatory cytokine to define the immune response generated by CPS-100 and CPS-400. Our preliminary findings suggested that CPS-100 is relatively more immunostimulatory in nature than immunoregulatory, as indicated by high IFNy and negligible IL-10 production (Fig. 8a-b). On the other hand, IFNy levels were undetectable in the TA fraction CPS-400 (Fig. 8a). To further confirm our hypothesis, we evaluated other cytokines in a similar set up by including tumor necrosis factor-α (TNF-α), interleukin 6 (IL-6), interleukin 12 (IL-12), interleukin 17 (IL-17) and interleukin 1β (IL1-β). CPS-100 stimulated cells to produce significantly high level of TNF-α, IL-6 and IL-12 (Fig. 8c-e) while IL-17 and IL-1β were not detected (data not shown). On the other hand, CPS-400 showed no apparent increase in any of the cytokines measured (Fig. 8c-e). To further address the issue of specificity of immunostimulatory response of CPS-100, we investigated if the IFN γ production was concentration dependent, as IFN γ is considered as the primary immunostimulatory marker produced by various types of immune cells. The calculated half maximal effective concentration (EC₅₀) of CPS-100 in IFN γ induction at 48 h was 3.16 μ M (Fig. 8f), suggesting CPS-100 can be regarded as an efficient immune stimulant. Future investigations into *in vivo* effects of CPS-100 and CPS-400 will define their specific immunomodulatory effects and their mechanisms

4. Discussion and conclusions

The aim of this study was to evaluate the nature of the carbohydrate components coating the surface of the probiotic bacterium, *L. plantarum* IMB19, and to gain preliminary information about their immunological role during the host-bacterium interaction.

First, it was found that this bacterium is coated with a complex mixture made of two teichoic acids (CPS-400), and of a capsular polysaccharide (CPS-100).

The repeating unit of CPS-100 comprises nine residues (five rhamnose, two galactose, one glucose and one N-acetylglucosamine) and it is joined to the next by a phosphodiester linkage (Fig. 6). Such large number of residues in a repeat is unusual as deduced by querying the Bacterial Carbohydrate Structure Database (Toukach & Egorova, 2016, last accessed in November 2019). Indeed, the number of polysaccharides having a repeat with nine residues is six, with 10 residues is 8, and only one for repeats with 10 or 11 sugars. Interestingly, most of the structures found are produced from probiotic bacteria, either *Lactobacilli* or *Bifidobacteria*, and none of them has a phosphate diester linkage, making the nature of CPS-100 from L. *plantarum* IMB19 unique, to the best of our knowledge.

Sugar composition of the CPS is distinct in comparison to previously

^{**} attributions can be reversed.

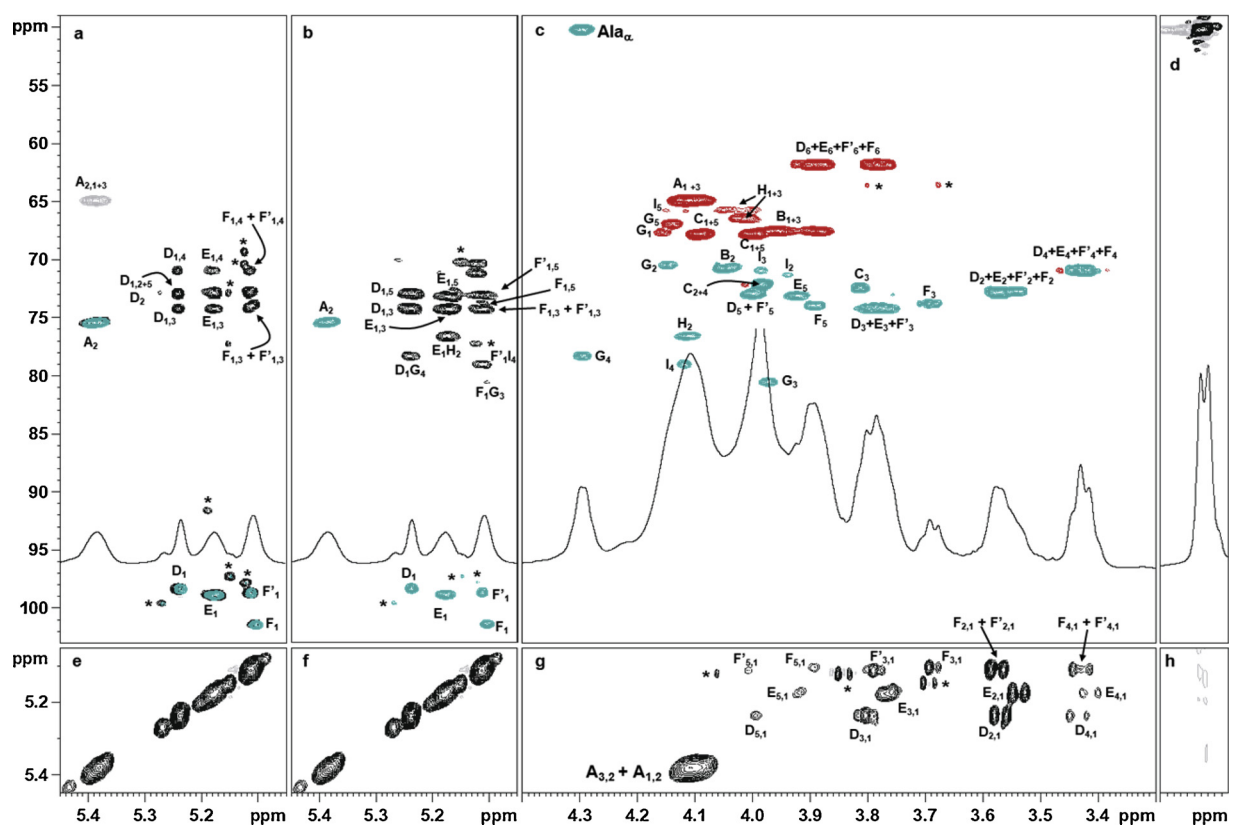


Fig. 7. (600 MHz, 310 K) NMR spectra recorded for CPS-400: a) overlay of HSQC-TOCSY (black) and HSQC (cyan); b) overlay of HMBC (black) and HSQC (cyan); c) HSQC; d) HSQC-TOCSY; e-h) different regions of the TOCSY spectrum. "*" densities belonging to unidentified minor motifs. Labels and the depiction of the structural units are reported in Table 2.

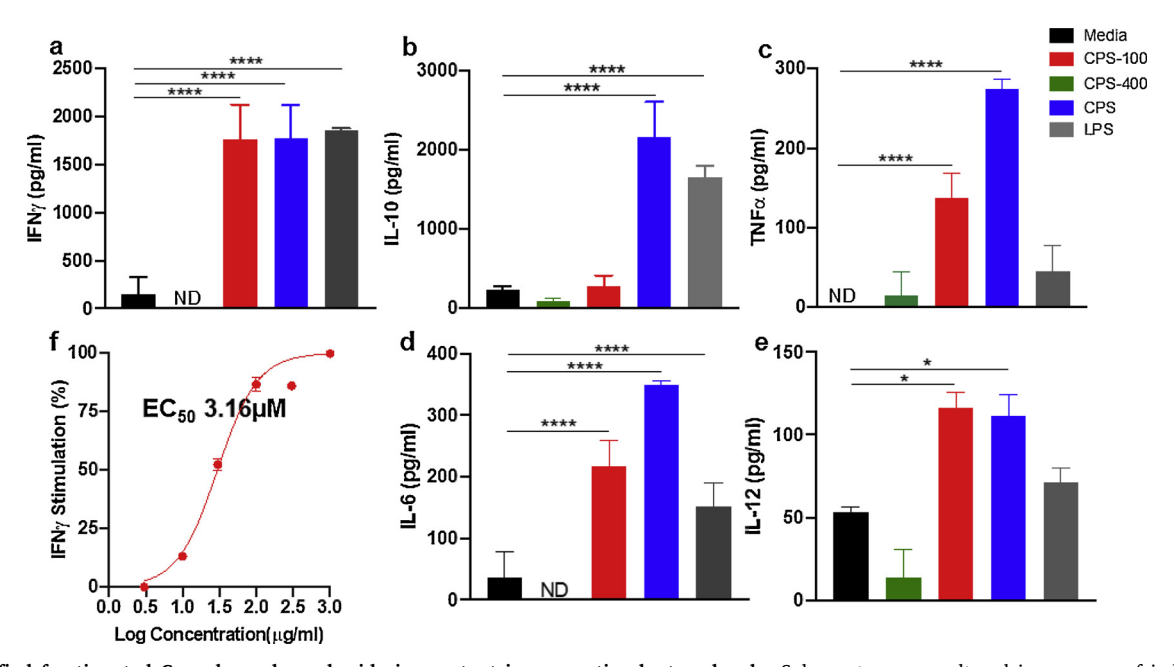


Fig. 8. Purified fractionated Capsular polysaccharide is a potent immuno-stimulant molecule. Splenocytes were cultured in presence of indicated polysaccharides, i.e. Media (without polysaccharide), fractionated (CPS-400 & CPS-100, 500 μ g/mL), total (CPS, 500 μ g/mL) and lipopolysaccharide (LPS from *E. coli* 0111:B4, 0.1 μ g/mL). Cell culture supernatants were then analyzed by ELISA for cytokine production. (a) IFN γ ; (b) IL-10; (c) TNF- α ; (d) IL-6; (e) IL-12; (f) Dose response curve for CPS-100 for IFN γ production with a calculated half maximal effective concentration (EC₅₀) as 3.16 μ M. Data are representative of two to three independent experiments with similar results. All bar graphs show the mean \pm SD. *p < 0.05, *****p < 0.0001 (*One-way ANOVA with post hoc Dunnet's test for multiple comparison*); ND, Not Detected.

reported strains of *L. plantarum*, with the exception of the strain TMW 1.1478 (Prechtl, Wefers, Jacob, & Vogel 2018), which also has glucose and galactose in the repeat but not glucosamine or phosphate, connected via a different sequence from that of our strain. Other studies have focused on the genetic composition and the immunological properties while the structural details have been ignored (Lee et al., 2016; Remus et al., 2012).

Secondly, we investigated the biological effects of the pure capsular polysaccharide (CPS-100) and of the teichoic acids (CPS-400) in relation to the effects triggered from total CPS fraction. On primary observation, it appeared that CPS induces significant IFN γ and IL-10 responses (Fig. 8b). Accordingly, we investigated the cytokine profiles induced from the two most representative fractions of the surface polysaccharides, CPS-100 and CPS-400, and we found that CPS-100 (Fig. 8) was the immunostimulatory component of CPS because of the remarkable effect in IFN γ production (EC $_{50}$ 3.157 μ M), including other cytokines, except IL-10. In contrast, CPS-400 had no activity in any of the assays (Fig. 8) so the nature of the IL-10 stimulation by unfractionated CPS is still elusive. Though indicative, these findings warrant an in-depth proof-of-concept immunological investigation of these molecules in health and disease.

In conclusion, our study demonstrates that the surface polysaccharides from a commensal microbiota related bacterium, L. *plantarum* IMB19 is a complex mixture made of teichoic acids and of a capsular polysaccharide. Such complexity is in line with the findings of other authors (Remus et al., 2012) including ourselves (Speciale et al., 2019), which report that the bacterial surface is covered by a complex blend of different carbohydrate polymers each with a different activity profile.

Our opinion is that the ability of bacteria to modulate the expression (and the amount) of each polymer, teichoic acid included (Brown et al., 2013; Remus et al., 2012), is the key for their adaptation to the host environment, and further studies are necessary to unravel this issue.

CRediT authorship contribution statement

Pilar Garcia-Vello: Formal analysis, Investigation, Writing - original draft. Garima Sharma: Formal analysis, Investigation, Writing - original draft. Immacolata Speciale: Formal analysis, Investigation. Antonio Molinaro: Formal analysis, Investigation, Writing - review & editing. Sin-Hyeog Im: Conceptualization, Formal analysis, Funding acquisition, Methodology, Project administration, Resources, Supervision, Writing - review & editing. Cristina De Castro: Conceptualization, Formal analysis, Funding acquisition, Methodology, Project administration, Resources, Supervision, Writing - review & editing.

Acknowledgements

P. G-V. fellowship is supported by the Train2Target project granted from the European Union's Horizon 2020 framework program for research and innovation (Project #721484)

Appendix A. Supplementary data

Supplementary material related to this article can be found, in the online version, at doi:https://doi.org/10.1016/j.carbpol.2020.115857.

References

Baarlen, P., Wells, J. M., & Kleerebezem, M. (2013). Regulation of intestinal homeostasis and immunity with probiotic lactobacilli. *Trends in Immunology, 34*, 208–215.
Bock, K., & Pedersen, C. (1983). Carbon-13 nuclear magnetic resonance spectroscopy of monosaccharides. *Advances in Carbohydrate Chemistry and Biochemistry, 41*, 27–65.
Bron, P. A., Tomita, S., van Swarm, I. I., Remus, D. M., Meijerink, M., Wels, M., et al. (2012). *Lactobacillus plantarum* possesses the capability for wall teichoic acid

- backbone alditol switching. Microbial Cell Factories, 11, 123-137.
- Brown, S., Santa Maria, J. P., Jr., & Walker, S. (2013). Wall teichoic acids of gram-positive bacteria. *Annual Review of Microbiology*, 67, 1–28.
- Chae, C. S., Kwon, H. K., Hwang, J. S., Kim, J. E., & Im, S. H. (2012). Prophylactic effect of probiotics on the development of experimental autoimmune myasthenia gravis. *PloS One.* 7, e52119.
- De Castro, C., Parrilli, M., Holst, O., & Molinaro, A. (2010). Microbe-associated molecular patterns in innate immunity: Extraction and chemical analysis of gram-negative bacterial lipopolysaccharides. *Methods in Enzymology*, 480, 89–115.
- Gerlach, D., Guo, Y., De Castro, C., Kim, S.-H., Schlatterer, K., Xu, F.-F., et al. (2018). Methicillin-resistant Staphylococcus aureus alters cell wall glycosylation to evade immunity. Nature, 563, 705–709.
- Górska, S., Schwarzer, M., Jachymek, W., Srutkova, D., Brzozowska, E., Kozakova, H., et al. (2014). Distinct immunomodulation of bone marrow-derived dendritic cell responses to Lactobacillus plantarum WCFS1 by two different polysaccharides isolated from Lactobacillus rhamnosus LOCK 0900. Applied and Environmental Microbiology, 80, 6506–6516.
- Kang, C. S., Ban, M., Choi, E. J., Moon, H. G., Jeon, J. S., Kim, D. K., et al. (2013). Extracellular vesicles derived from gut microbiota, especially Akkermansia muciniphila, protect the progression of dextran sulfate sodium-induced colitis. Proceedings of the National Academy of Sciences of the USA, 8, e76520.
- Kleerebezem, M., Hols, P., Bernard, E., Rolain, T., Zhou, M., Siezen, R. J., et al. (2010). The extracellular biology of the lactobacilli. FEMS Microbiology Reviews, 34, 199–230.
- Kwon, H. K., Lee, C. G., So, J. S., Chae, C. S., Hwang, J. S., Sahoo, A., et al. (2010). Generation of regulatory dendritic cells and CD4⁺Foxp3⁺ t cells by probiotics administration suppresses immune disorders. Proceedings of the National Academy of Sciences of the USA, 107, 2159–2164.
- Lancefield, R. C. (1933). A serological differentiation of human and other groups of hemolytic streptococci. The Journal of Experimental Medicine, 57, 571–595.
- Lee, I. C., Caggianiello, G., Swam, I. R. V., Taverne, N., Meijerink, M., Bron, P. A., et al. (2016). Strain-specific features of extracellular polysaccharides and their impact on Lactobacillus plantarum-Host interactions. Applied and Environmental Microbiology, 82, 3959–3970.
- Prechtl, R. M., Wefers, D., Jacob, F., & Vogel, F. R. (2018). Structural characterization of the surface-associated heteropolysaccharide of *Lactobacillus plantarum* TMW 1.1478 and genetic analysis of its putative biosynthesis cluster. *Carbohydrate Polymers*, 202, 236–245.
- Remus, D. M., Kranenburg, R. V., Swam, I. R. V., Taverne, N., Bongers, R. S., Wels, M., et al. (2012). Impact of 4 *Lactobacillus plantarum* capsular polysaccharide clusters on surface glycan composition and host cell signaling. *Microbial Cell Factories*, 11, 149–151.
- Rocha-Ramírez, L. M., Pérez-Solano, R. A., Castañón-Alonso, S. L., Moreno Guerrero, S. S., Ramírez Pacheco, A., García Garibay, M., et al. (2017). Probiotic Lactobacillus strains stimulate the inflammatory response and activate human macrophages. *Journal of Immunological Research*, 2017, 4607491.
- Sanchez, J. I., Martinez, B., Guillen, R., enez-Diaz, R. F., & Rodriguez, A. (2006). Culture conditions determine the balance between two different exopolysaccharides produced by Lactobacillus pentosus LPS26. Applied and Environmental Microbiology, 72, 7495–7502.
- Sechenkova, S. N., Perepelov, A. V., Cedzynski, M., Swierzko, A., Ziolkowski, A., Shashkov, A. S., et al. (2004). Structure of a highly phosphorylated O-polysaccharide of *Proteus mirabilis* O41. Carbohydrate Research, 339, 1347–1352.
- Shashkov, A. S., Potekina, N. V., Senchenkova, S. N., & Kudryashova, E. B. (2009). Anionic polymers of the cell wall of *Bacillus subtilis* subsp. *Subtilis* VKM B-501. *Biochemistry (Moscow)*, 74, 543–548.
- Speciale, I., Verma, R., Di Lorenzo, F., Molinaro, A. B., Im, S. H., & De Castro, C. (2019). Bifidobacterium bifidum presents on the cell surface a complex mixture of glucans and galactans with different immunological properties. Carbohydrate Polymers, 218, 269–278
- Streshinskaya, G. M., Shashkov, A. S., Potekhina, N. V., Kozlova, Y. I., Tul'skaya, E. M., Senchenkova, S. N., et al. (2011). Carbohydrate-containing cell wall polymers of some strains of the *Bacillus subtilis* group. *Microbiology*, 80, 21–29.
 Telesford, K. M., Yan, W., Ochoa-Reparaz, J., Pant, A., Kircher, C., Christy, M. A., et al.
- Telesford, K. M., Yan, W., Ochoa-Reparaz, J., Pant, A., Kircher, C., Christy, M. A., et al (2015). A commensal symbiotic factor derived from *Bacteroides fragilis* promotes human CD39(+)Foxp3(+) T cells and Treg function. *Gut Microbes*, 6, 234–242.
- Tomita, S., Furihata, K., Nukada, T., Satoh, E., Uchimira, T., & Okada, S. (2009). Structures of two monomeric units of teichoic acid prepared from the cell wall of Lactobacillus plantarum NRIC 1068. Bioscience, Biotechnological, and Biochemistry, 73, 530–535.
- Tomita, S., Tanaka, N., & Okada, S. (2017). A rapid method-based for discrimination of strain-specific cell wall teichoic acid structures reveals a third backbone type in *Lactobacillus plantarum. FEMS Microbiology Letters, 364*, 1–10.
- Torriani, S., Felis, G. E., & Dellaglio, F. (2001). Differentiation of Lactobacillus plantarum, L. pentosus, and L. paraplantarum by recA gene sequence analysis and multiplex PCR assay with recA gene-derived primers. Applied and Environmental Microbiology, 67(8), 3450–3454.
- Toukach, P. V., & Egorova, K. S. (2016). Carbohydrate structure database merged from bacterial, archaeal, plant and fungal parts. *Nucleic Acids Research*, 44(D1), D1220-D1236
- Valueva, O. A., Shashkov, A. S., Zdorovenko, E. L., Chizhov, A. O., Kiseleva, E., Novik, G., et al. (2013). Structures of cell-wall phosphate-containing glycopolymers of *Bifidobacterium longum* BIM B-476-D. *Carbohydrate Research*, 373, 22–27.
- Verma, R., Lee, C., Jeun, E. J., Yi, J., Kim, K. S., Ghosh, A., et al. (2018). Cell surface polysaccharides of Bifidobacterium bifidum induce the generation of Foxp3 + regulatory T cells. Science Immunology, 19(3(28)).
 Zeidan, A. A., Poulsen, V. K., Janzen, T., Buldo, P., Derkx, P. M. F., Øregaard, G., et al.
- Zeidan, A. A., Poulsen, V. K., Janzen, T., Buldo, P., Derkx, P. M. F., Øregaard, G., et al. (2017). Polysaccharide production by lactic acid bacteria: From genes to industrial applications. FEMS Microbiology Reviews, 41, S168–S200.